Liver INTERNATIONAL
OFFICIAL JOURNAL OF THE INTERNATIONAL ASSOCIATION FOR THE STUDY OF THE LIVER

Liver International ISSN 1478-3223

CLINICAL STUDIES

Intrahepatic cholangiocarcinomas in cirrhosis are hypervascular in comparison with those in normal livers

Jing Xu[1,5†], Saya Igarashi[1,2†], Motoko Sasaki[1], Takashi Matsubara[1,2], Norihide Yoneda[1,2], Kazuto Kozaka[2], Hiroko Ikeda[3], Jihun Kim[4], Eunsil Yu[4], Osamu Matsui[2] and Yasuni Nakanuma[1]

1 Department of Human Pathology, Kanazawa University Hospital, Kanazawa, Japan
2 Department of Radiology, Kanazawa University Graduate School of Medicine, Kanazawa, Japan
3 Section of Diagnostic Service of Pathology, Kanazawa University Hospital, Kanazawa, Japan
4 Department of Pathology, University of Ulsan College of Medicine Asan Medical Center, Seoul, South Korea
5 Department of Pathology, Shanxi Medical University, Taiyuan, China

Keywords
cirrhosis – combined hepatocellular and cholangiocarcinoma – dynamic imaging – Intrahepatic cholangiocarcinoma – tumour vasculature

Correspondence
Yasuni Nakanuma, MD, Department of Human Pathology, Kanazawa University Graduate School of Medicine, Kanazawa 920-8640, Japan
Tel: +81-76-265-2197
Fax: +81-76-234-4229
e-mail: pbcpsc@kenroku.kanazawa-u.ac.jp

Received 27 October 2011
Accepted 14 February 2012

DOI:10.1111/j.1478-3231.2012.02783.x

Abstract

Background and Aims: Intrahepatic cholangiocarcinomas (ICCs) are usually adenocarcinomas with fibrotic and hypovascular stroma. Intrahepatic cholangiocarcinomas in cirrhosis and precirrhotic liver (ICC-cirrhosis) are increasingly being diagnosed, and can display hypervascluar enhancement resembling a hepatocellular carcinoma on dynamic imaging. *Methods:* In this study using ICC-cirrhosis (71 cases), ICC with non-specific reactive changes (ICC-reactive) (72 cases) and the cholangiocarcinoma component of combined hepatocellular cholangiocarcinoma (HCC-ICC) (30 cases), we tried to compare the tumour vasculature. *Results:* It was found that ICC-cirrhosis and the cholangiocarcinoma component of HCC-ICC showed a higher density of arteries and microvessels ($1.59 \pm 0.58/mm^2$ (mean ± SD) and $140 \pm 43/mm^2$ in ICC-cirrhosis and $1.74 \pm 0.67/mm^2$ and $131 \pm 46/mm^2$ in the cholangiocarcinoma component of HCC-ICC) than in ICC-reactive ($1.26 \pm 0.61/mm^2$ and $103 \pm 45/mm^2$). Dynamic computed tomography (CT) and magnetic resonance imaging (MRI) showed that a majority of ICC-cirrhosis displayed strong hypervascular enhancement, whereas one-third of ICC-reactive each showed strong, weak and no or minimal enhancement respectively. The increased vascular density was positively correlated with enhanced arterial phase of dynamic CT and MRI. *Conclusion:* The density of arteries and microvessels of ICC-cirrhosis was higher than that in ICC-reactive and comparable to that in the cholangiocarcinoma component of HCC-ICC, and the higher density of arteries and microvessels in ICC may be responsible for the hypervascular enhancement of ICC-cirrhosis.

Intrahepatic cholangiocarcinoma (ICC), a primary liver malignancy secondary to hepatocellular carcinoma (HCC), arises from the intrahepatic bile ducts and affects adults of both gender (1,2). Although the majority of ICCs develop in apparently normal livers, several risk factors have been suggested (1,3). The best known of these are chronic biliary diseases, such as primary sclerosing cholangitis (PSC) and hepatolithiasis (1,4). Lately, cirrhosis, mainly caused by chronic infection with hepatitis C virus (HCV), has been recognized as an important risk factor for ICC and this association has been speculated as the cause of the increasing incidence of ICC in recent years (5–7). However, very few studies have described the clinicopathological features of ICC in cases of cirrhosis (8–11).

ICC is usually a well to moderately-differentiated adenocarcinoma with fibrotic and hypovacular stroma (1,2,12,13). Angiographically, ICC typically displays a hypovascular mass with or without peripheral enhancement and these features are mainly obtained from ICC cases arising in non-cirrhotic livers (14,15). However, the vasculature of ICCs is not always uniform pathologically and angiographically. For example, some cases show an enhancement in the arterial phase identical to that in HCC (16). Recent findings, using contrast-enhanced ultrasonography (CEUS), indicated that ICC in cirrhosis shared a similar pattern of enhancement with HCC, which makes the diagnosis of ICC more complex (8,17). So far, the characteristic pathological features including the tumour vasculature

†Dr. Jing Xu and Dr. Saya Igarashi contributed equally to this study.

in ICC, in patients with cirrhosis have yet to be clarified with respect to such angiographical characteristics.

Herein, we tried to characterize the vasculature in ICC with respect to background lesions, by comparing numbers (density) of arteries and microvessels in cases of ICC in non-biliary cirrhosis and precirrhotic liver (ICC-cirrhosis), with those in cases of ICC in livers showing a normal histology or non-specific reactive changes (ICC-reactive) and also with those in cholangiocarcinoma (CC) components of combined hepatocellular and cholangiocarcinoma (HCC-ICC). In addition, in selected cases of ICC in which dynamic computed tomography (CT) and magnetic resonance imaging (MRI) were done, we evaluated the arterial (early) phases of ICC-cirrhosis and ICC-reactive, and tried to correlate the vascular patterns with the number (density) of vasculatures.

Materials and methods

Case selection and tissue preparation

A total of 173 liver tissue specimens (143 cases of ICC and 30 cases of HCC-ICC) were collected from the surgical and autopsy files of the Department of Human Pathology, Kanazawa University Graduate School of Medicine and affiliated hospitals (137 cases) (1990–2010) and the surgical files of the Department of Pathology, University of Ulsan College of Medicine, Asan Medical center, Korea (36 cases) (1996–2009). They were composed of 32 autopsied specimens, 140 surgical specimens and one wedge biopsy specimen. Autopsy cases (32 cases) were consecutively obtained from the autopsy file done in the Department of Human Pathology, Kanazawa University Graduate School of Medicine and 105 surgical cases of ICC including one wedge biopsy and 36 surgical cases were also consecutively collected from Kanazawa University and Asan Medical Center respectively. Among 143 ICC cases, the surrounding liver of 72 cases of ICC showed nonspecific reactive change (ICC-reactive) [men and women; 45; 27, age distribution 35–93 (mean 65)] and that of 71 cases of ICC showed ICC-cirrhosis [men and women; 50; 21, age distribution 37–85 (mean 60)] [25 cases owing to hepatitis B viral infection, 14 cases to hepatitis C viral infection, 1 case caused by a double infection, 2 cases associated with alcoholic steatohepatitis, 17 cases with non-alcoholic steatohepatitis (NASH) and 12 cases of unknown aetiology]. All cases of Asan Medical Center (36 cases) were ICC-cirrhosis consecutively chosen from the surgical file (1996–2009). The remaining 137 cases of ICC and 30 cases of HCC-CCC of Kanazawa University were consecutively obtained from autopsy and surgical files (1990–2010). Among 30 cases of HCC-ICC, 27 cases were associated with cirrhosis or precirrhotic liver and three cases with NSR; each tended to show a similar gender and age distribution to ICC-cirrhosis and ICC-reactive respectively. ICCs are largely classifiable into peripheral and perihilar types (2,13). Peripheral ICCs presumably develop from the intrahepatic small bile duct and bile ductules, and usually show a mass-forming growth (1). Perihilar ICCs involve the intrahepatic large bile duct and hilar ducts and are usually of the periductal spreading type. Sixty-nine and two cases were of the peripheral type and the perihilar type, respectively, in 71 ICC-cirrhosis. Sixty-five and seven cases were the peripheral type and the perihilar type, respectively, in 72 ICC-reactive. Sixty-three cases were macroscopically mass-forming type and the remaining eight were periductal infiltrating type in 71 ICC-cirrhosis. Fifty-five, eight and eleven cases were mass-forming type, mass-forming + periductal infiltrating type, and periductal infiltrating type, respectively, in ICC-reactive.

Histologically, ICC-reactive or ICC-cirrhosis and CC components of HCC-ICC were adenocarcinomas showing tubular, acinar, papillary, solid or cord-like patterns in combination with various fibrous and inflammatory stroma. In this study, we did not examine anaplastic or sarcomatous elements and squamous cell carcinomas, even if present. Sixty and 11 cases were well to moderately differentiated and poorly differentiated adenocarcinoma, respectively, in 71 ICC-cirrhosis. Sixty-four and eight cases were well to moderately differentiated and poorly differentiated adenocarcinoma, respectively, in 72 ICC-reactive.

All of these tissue samples were fixed in 10% neutral buffered formalin and embedded in paraffin. Two or three blocks showing a representative histology of carcinoma and background liver were selected in each case for further examination. More than 20 consecutive 4-μm-thick sections were cut from each paraffin block and stained with haematoxylin and eosin (H&E) and Elastica van Gieson (EVG) stain for identification of the arterial architecture with the elastic lamina.

Immunohistochemistry

Immunostaining of CD34 was used for the identification of vascular endothelial cells (18). In brief, after the blocking of endogenous peroxidase and incubation in normal goat serum (1:10; Vector Laboratories, Burlingame, CA, USA) for 20 min, the deparaffinized sections were incubated overnight at 4°C with a primary mouse monoclonal antibody against CD34 (clone QBEnd10; 1:200; Beckman Coulter, Brea, CA, USA). The sections were then incubated at room temperature for 1 h with goat anti-mouse immunoglobulins conjugated to a peroxidase labelled-dextran polymer (EnVisionC; Dako Cytomation, Carpinteria, CA, USA). The reaction products were developed by immersing the sections in a 3, 3′-diaminobenzidine tetrahydrochloride (DAB) solu-

tion containing 0.03% hydrogen peroxide. Nuclei were lightly counterstained with haematoxylin.

Semiquantitative evaluation of the vasculature within stroma of ICC

The density of arteries and microvessels within the stroma of ICC were semiquantitatively evaluated in 72 cases of ICC-reactive, 71 cases of ICC-cirrhosis and 30 cases of HCC-ICC described elsewhere, as follows.

Densities of arteries

In three low power fields (at ×100; each area was 2.5434 mm^2) selected at random from different parts in the central area of the tumour's stroma, the number of arteries with elastic lamina (Fig. 1A) was counted. The average numbers in three fields was regarded as the arterial density.

Density of microvessels

In five high power fields (at ×400; each area was 0.1589 mm^2) selected at random from different parts in the central area of the stroma, the number of CD34-positive microvessels (Fig. 1B) without an elastic lamina, including capillaries, was counted. The average number in these five fields was regarded as the microvessel density.

Imaging studies

To evaluate the vasculature of ICCs radiologically, among the 72 cases of ICC-reactive and 71 cases of ICC-cirrhosis in which the histopathological semiquantitative analyses were performed, the cases in which dynamic CT and dynamic MRI were done at Kanazawa University Hospital, were chosen retrospectively and consecutively. Then, the arterial dominant phase images were evaluated in the chosen cases blindly by three radiologists (K. Kozaka, N.Yoneda and S.Igarashi).

CT Imaging

Eleven cases of ICC-cirrhosis and 23 cases of ICC-reactive which were included in the pathological evaluation had undergone dynamic contrast-enhanced CT at Kanazawa University Hospital. CT imaging was performed using 4-, 16- and 64-detector row CT scanners (LightSpeed Plus, Ultra 16 and VCT; GE Medical Systems, Milwaukee, WI, USA). The parameters

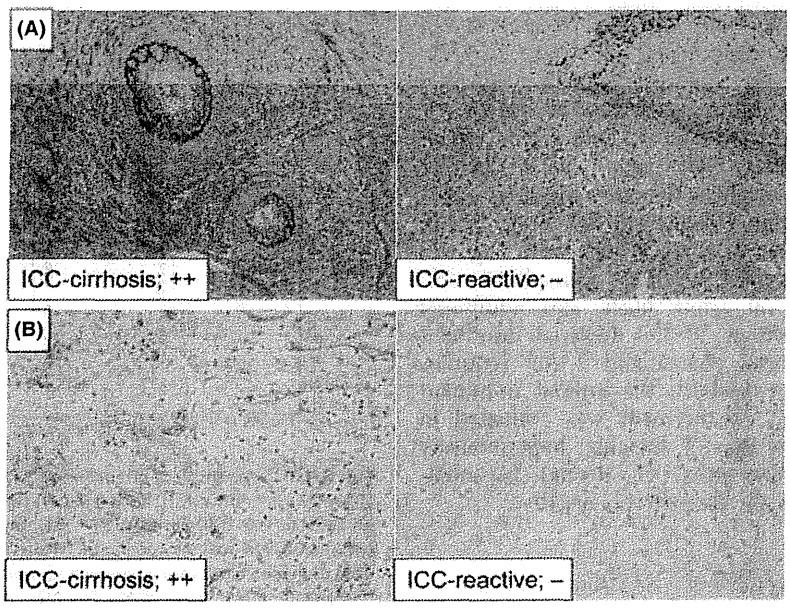

Fig. 1. (A) Arteries with elastic lamina in the tumour tissue of ICC are found in the stroma of intrahepatic cholangiocarcinoma. Elastica van Gieson (EVG) stain. ×100. Left, a representative case of intrahepatic cholangiocarcinoma (ICC) arising in non-biliary, cirrhosis of precirrhotic liver (ICC-cirrhosis) in which the enhancement during the early phase was classified as strong (++) in dynamic CT and MRI. Right, ICC with non-specific reactive change (ICC-reactive) in which the enhancement during the early phase was classified as negative (–) in dynamic CT and MRI. (B) Microvessels positive for CD34 in the stroma of intrahepatic cholangiocarcinoma are identified by CD34 immunostaining. Immunostaining of CD34 and haematoxylin, ×400. Left, a representative case of intrahepatic cholangiocarcinoma (ICC) arising in non-biliary, cirrhosis of precirrhotic liver (ICC-cirrhosis) in which the enhancement during the early phase was classified as strong (++) in dynamic CT and MRI. Right, ICC with non-specific reactive change (ICC-reactive) in which the enhancement during the early phase was classified as negative (–) in dynamic CT and MRI.

were section thickness; 2.5 mm, tube voltage; 120 kV and tube current; auto mA at VCT, 250–300 mA at Light Speed Plus and Ultra 16. After precontrast CR scans were obtained, triple phasic in 4 patients, quadruple phasic in 28 patients and octuplet phasic dynamic study in 2 patients were done. In this study, we adapted and evaluated early and delayed phase among these images. Early phase was defined as follows: hepatic arteries and portal veins were well enhanced, but the enhancement was stronger in hepatic arteries than portal veins. Delayed phase was defined as follows: hepatic arteries, portal veins and hepatic veins showed the same degree of contrast enhancement.

Enhancement in the arterial dominant phase was evaluated within the slice containing the largest cross-section of the tumour. If the tumour showed ring-like enhancement, the necrotic areas where there were no enhancement in the delayed phase were excluded. Comparing to the non-cancerous areas, enhancement patterns were classified as showing high-density relative to surrounding areas (++, strong), iso-density (+, weak) and low-density (–, negative).

MR Imaging

For 12 cases of ICC-cirrhosis and 17 cases of ICC-reactive, MRI was performed using a 1.5T (n = 15) or 3.0T (n = 16) unit (Signa Horizon, EXCITE HDxt; GE Medical Systems, Milwaukee, WI, USA) and T1-weighted imaging was obtained with the 2D-Fast SPGR at a slice-thickness of 5 mm or LAVA-XV sequence at a slice-thickness of 4.2 mm and a gap of 2.1 mm. The matrix size was 256 × 128 or 256 × 256. For T1-weighted dynamic imaging, gadopentetate dimeglumine (Magnevist; Schering, Berlin, Germany) was injected as a rapid bolus with a power injector at a dose of 0.1 mmol/kg, immediately followed by a 10–20 ml saline flush, and additional images were obtained at 30–35 s (arterial dominant phase), 65–70 s (portal phase) and 3 min (equilibrium phase). In our analysis, the arterial dominant phase was used and enhancement was evaluated in the same way as for the CT imaging; hyperintensity relative to surrounding areas (++, strong), iso-intensity (+, weak) and hypo-intensity (–, negative).

Statistical analysis

Numerical data were presented as the mean ± standard deviation (SD). Data from different groups were compared using a one-way analysis of variance and examined using the Kruskal–Wallis test followed by Dunn's post test. Differences in the proportions of categorical data were tested using the Chi-square test. The correlation coefficient of two factors was evaluated using Spearman's rank correlation test. The results were considered significant if the P value was < 0.05.

Results

Semiquantitative evaluation of the vasculature within tumours

Arterial density

As shown in Fig. 2A, the arterial density within tumours was higher in the 72 ICC-cirrhosis (mean ± SD: 1.59 ± 0.58/mm^2 and range: 0.63–3.15/mm^2) and 30 cases of the CC component of HCC-ICC (1.74 ± 0.67/

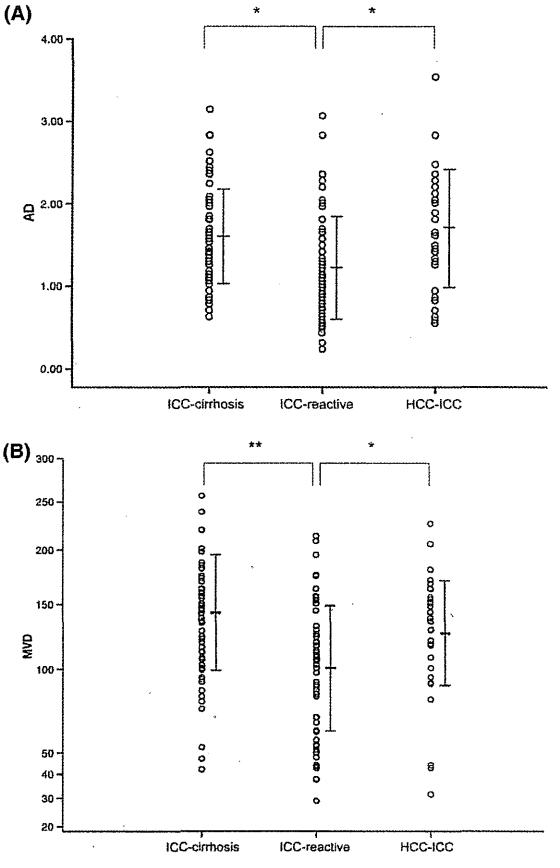

Fig. 2. (A) Comparison of arterial density (AD) among intrahepatic cholangiocarcinoma (ICC) arising in non-biliary, cirrhosis and precirrhotic liver (ICC-cirrhosis) (n = 71), the CC component of hepatocellular cholangiocarcinoma (HCC-CCC) (n = 30) and ICC with non-specific reactive change (ICC-reactive) (n = 72); Data are displayed in scatter plots of AD. The AD is higher in ICC-cirrhosis and the CC component of HC-CC than in ICC-reactive. The bar shows mean ± SD; P < 0.01. (B) Comparison of microvessel density (MVD) among intrahepatic cholangiocarcinoma (ICC) arising in cirrhosis and precirrhotic liver (ICC-cirrhosis) (n = 72), the CC component of hepatocellular cholangiocarcinoma (HCC-CCC) (n = 30) and ICC with non-specific reactive change (ICC-reactive) (n = 7). Data are displayed in scatter plots of AD. Data are displayed in scatter plots of MVD; the bar shows the mean ± SD. The MVD is higher in ICC-cirrhosis and in the CC component of HCC-CCC than in ICC-reactive; P < 0.05; P < 0.001.

mm^2 and 0.55–3.54/mm^2) than in ICC-reactive (1.26 ± 0.61/mm^2 and 0.24–3.07/mm^2 respectively) ($P < 0.01$ and $P < 0.01$ respectively). The arterial density was not different between ICC-cirrhosis and the cholangiocarcinoma component of HCC-ICC ($P > 0.05$). The mean arterial density was not different between well to moderately differentiated and poorly differentiated adenocarcinoma ($P > 0.05$)(data not shown).

Microvessel density

As shown in Fig. 2B, the microvessel density within tumours was higher in ICC-cirrhosis (mean ± SD: 140 ± 43/mm^2 and range: 42–256/mm^2) and in the cholangiocarcinoma component of HCC-ICC (131 ± 46/mm^2 and 31–227/mm^2) than in ICC-reactive (103 ± 45/mm^2 and 29–214/mm^2) ($P < 0.001$ and $P < 0.05$ respectively). The mean microvessel density was not different between well to moderately differentiated and poorly differentiated adenocarcinoma ($P > 0.05$)(data not shown).

Imaging studies

The distribution of the arterial dominant phase images of dynamic CT and MRI are shown in Table 1. The representative images of dynamic CT and MRI in ICC-cirrhosis and ICC-reactive are shown in Fig. 3.

Dynamic CT

Enhancement during the early phase in 11 cases of ICC-cirrhosis was classified as follows:++, nine cases;+, two cases; and -, zero case. That in eight cases of ICC-reactive was classified as++, eight cases;+, nine cases; and -, six cases. Almost all cases of ICC-cirrhosis showed strong enhancement in the early phase, whereas about one-third of ICC-reactive cases showed strong enhancement, one-third showed mild enhancement and the remaining third showed no or minimum enhancement ($P < 0.01$).

Dynamic MRI

The early phase in 12 cases of ICC-cirrhosis was classified as follows: ++, ten cases; +, one case; and –, one case. Seventeen cases of ICC-reactive were classified as ++, six cases; +, six cases; and –, five cases. Almost all cases of ICC-cirrhosis showed strong enhancement in the early phase, whereas about one-third of ICC-reactive cases showed strong enhancement, one-third showed mild enhancement and the remaining third showed no or minimum enhancement ($P < 0.01$).

Correlation between the imaging and semiquantitative pathological evaluation

Dynamic CT and semiquantitative evaluation

As shown in Fig. 4A, the arterial density in nine cases of ICC with strong enhancement (++) was 1.51 ± 0.47/mm^2 (mean ± SD) with a range 0.94–2.4/mm^2, that in 14 cases of ICC with weak enhancement was 1.25 ± 0.57/mm^2 (mean ± SD) with a range 0.53–2.20/mm^2 and that in four cases of ICC with no or minimum enhancement was 0.88 ± 0.25/mm^2 (mean ± SD) with a range 0.57–1.13/mm^2. ICC cases with stronger enhancement showed higher arterial density ($P < 0.01$, $r = 0.437$).

As shown in Fig. 4B, the microvascular density in nine cases of ICC with strong enhancement (++) was 134.4 ± 27.1/mm^2 (mean ± SD) with a range of 91.2–187.5/mm^2, that in 14 cases of ICC with weak enhancement was 117.4 ± 48.8/mm^2 (mean ± SD) with a range of 37.8–239.1/mm^2 and that in four cases of ICC with no or minimum enhancement was 97.4 ± 44.0/mm^2 (mean ± SD) with a range of 44.1–151.0/mm^2. ICC cases with stronger enhancement showed higher microvessel density ($P < 0.01$, $r = 0.444$).

Dynamic MRI and semiquantitative evaluation

As shown in Fig. 5A, the arterial density in 16 cases of ICC with strong enhancement (++) was 1.56 ± 0.52/mm^2 (mean ± SD) with a range of 0.79–2.40/mm^2, that in seven cases of ICC with weak enhancement was 1.13 ± 0.46/mm^2 (mean ± SD) with a range of 0.53–2.01/mm^2 and that in six cases of ICC with no or minimum enhancement was 1.01 ± 0.44/mm^2 with a range of 0.53–1.65/mm^2. Intrahepatic cholangiocarcinomas cases with stronger enhancement showed higher arterial density ($P < 0.01$, $r = 0.509$).

Table 1. The distribution of the arterial (early) phase images of dynamic computed tomography (CT) and magnetic resonance imaging (MRI) in intrahepatic cholangiocarcinoma (ICC) arising in non-biliary cirrhosis and precirrhotic liver (ICC-cirrhosis) and ICC with non-specific reactive change (ICC-reactive)

	CT			MRI		
	ICC-cirrhosis (n = 11)	ICC-reactive (n = 23)	P	ICC-cirrhosis (n = 12)	ICC-reactive (n = 17)	P
Early phase			<0.01			<0.05
++	9	8		10	6	
+	2	9		1	6	
–	0	6		1	5	

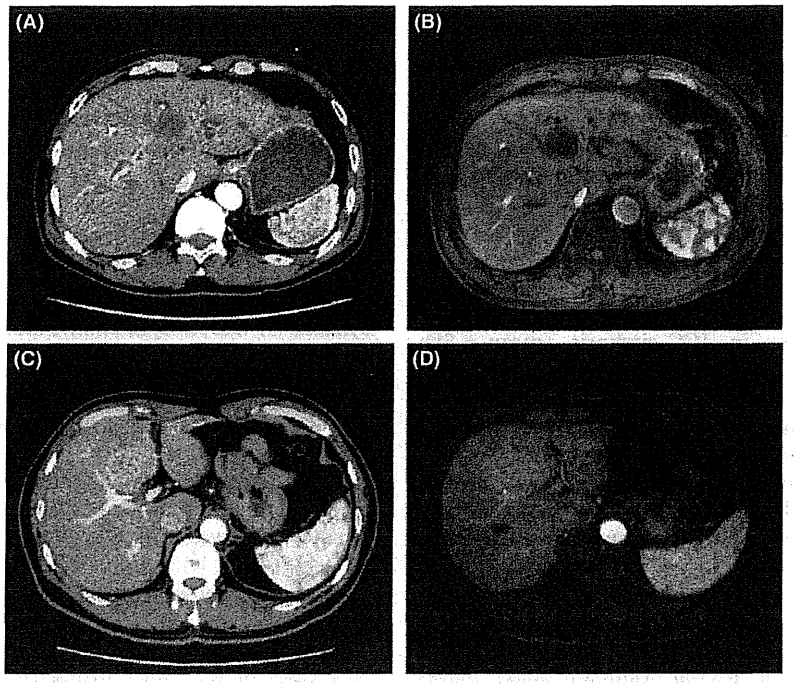

Fig. 3. Dynamic computed tomography of intrahepatic cholangiocarcinoma arising in a liver with non-specific reactive change. No or minimum enhancement is found in the early (arterial) phase of the tumour (arrow). (B) Dynamic magnetic resonance imaging of intrahepatic cholangiocarcinoma arising in a liver with non-specific reactive change. No or minimum enhancement is found in the early (arterial) phase of the tumour (arrow). Fig. 3A and 3B are from the same case at the same point in time of examination. (C) Dynamic computed tomography of intrahepatic cholangiocarcinoma arising in a liver with cirrhosis related to hepatitis C viral infection. Strong enhancement is found in the early (arterial) phase of the tumour (arrow). (D) Dynamic magnetic resonance imaging of intrahepatic cholangiocarcinoma arising in a liver with cirrhosis related to hepatitis C viral infection. Strong enhancement is found in the early (arterial) phase of the tumour (arrow). Fig. 3C and 3D are from the same case at the same point in time of examination.

As shown in Fig. 5B, the microvessel density in 16 cases of ICC with strong enhancement (++) was 142.5 ± 40.0/mm^2 (mean ± SD) with a range 91.3–239/mm^2, that in seven cases of ICC with weak enhancement was 107.3–36.8/mm^2 (mean ± SD) with a range 37.7–154.0/mm^2 and that in six cases of ICC with no or minimum enhancement was 109.7 ± 26.2/mm^2 with a range 86.2–156.1/mm^2. Intrahepatic cholangiocarcinomas cases with stronger enhancement showed higher microvessel density ($P < 0.01$, $r = 0.488$).

Discussion

The findings of this study can be summarized as follows: (i) the number (density) of arteries and microvessels within the tumour stroma are similar in ICC-cirrhosis and cholangiocarcinoma components of HCC-ICC and both of them are higher than that in ICC-reactive; (ii) dynamic CT and MRI showed that a majority of ICC-cirrhosis were hypervascular, whereas ICC-reactive were variable; (iii) the density of arteries and microvessels correlated with the degree of increased enhancement in ICCs shown by the arterial phase of dynamic CT and MRI.

Angiographically, ICCs tend to display a hypovascular mass, and CT and MRI often show hypovascular enhancement (4,19–22). However, these pathological and angiographical features are mainly based on ICCs arising in normal livers. In fact, Nanashima *et al.*, using CT, showed that ICCs arising in cases of chronic viral hepatitis frequently showed a hyperenhanced rather than hypoenhanced pattern (16). Recently, Vilana *et al.*, using CEUS and MRI, revealed that all the tumour nodules in ICCs in patients with cirrhosis showed contrast enhancement at the arterial phase, followed by contrast washout in venous phases, thus being totally indistinguishable from HCC (8,17). The characteristics of the tumour vasculature in ICC-cirrhosis have yet to be clarified.

In recent years, ICC has been found increasingly in patients with cirrhosis and distinguishing it from HCC is a major clinical issue because the prognosis and treatment options differ significantly between the two (8,14,17). Upon the detection of a suspicious nodule, a strategy based on dynamic imaging should be initiated, although detailed information is needed to characterize and diagnose ICC in cases of cirrhosis by dynamic CT and MRI and pathological and radiological correlations are limited at present.

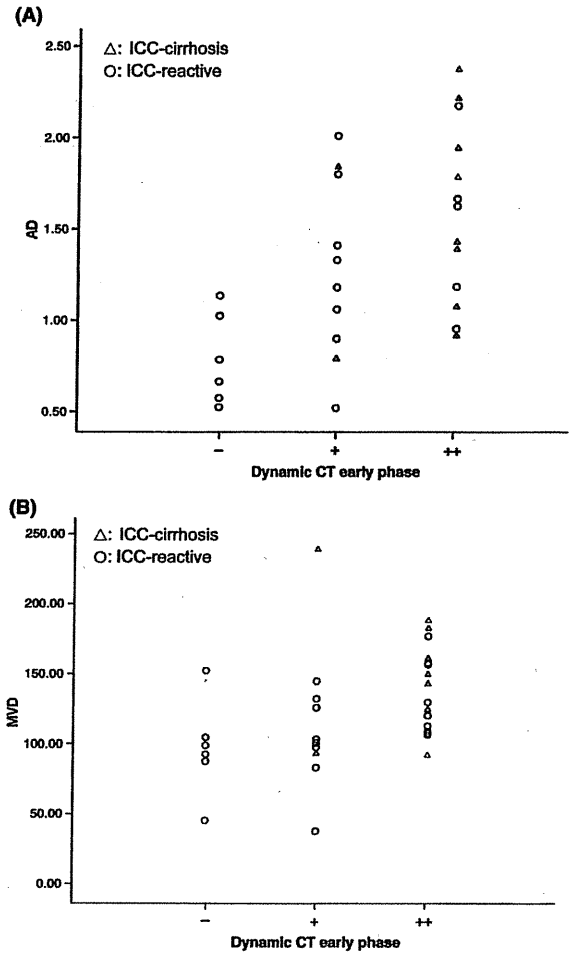

Fig. 4. (A) The correlation between the arterial phase enhancement of intrahepatic cholangiocarcinoma (ICC) in computed tomography (CT) and arterial density (AD) in ICC with cirrhosis and precirrhotic liver (ICC-cirrhosis) (△) and with non-specific reactive change (ICC-reactive) (○). The enhancement of the arterial phase of ICC is correlated with AD ($P < 0.01$, $r = 0.437$). –, no or minimum enhancement; +, mild enhancement; and ++, strong enhancement. (B) The correlation between the arterial phase enhancement of intrahepatic cholangiocarcinoma (ICC) in magnetic resonance imaging (MRI) and microvessel density (MVD) in intrahepatic cholangiocarcinoma with cirrhosis and precirrhotic liver (ICC-cirrhosis) (△) and with non-specific reactive change (ICC-reactive) (⊙). The enhancement in the arterial phase and the ICC tumour is correlated with MVD ($P < 0.01$, $r = 0.444$). –, no or minimum enhancement; +, mild enhancement; and ++, strong enhancement.

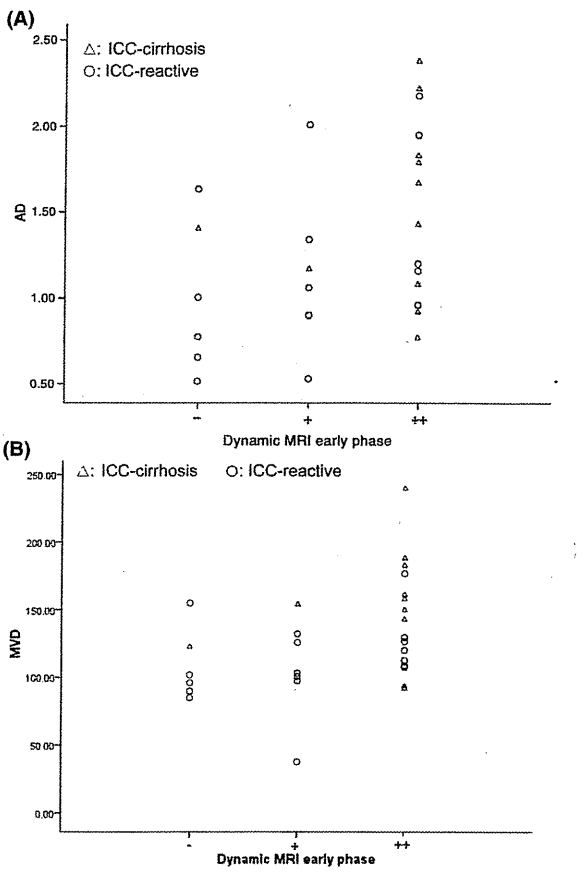

Fig. 5. (A) The correlation between the arterial phase enhancement of intrahepatic cholangiocarcinoma (ICC) in computed tomography (CT) and arterial density (AD) in intrahepatic cholangiocarcinoma with cirrhosis and precirrhotic liver (ICC-cirrhosis) (△) and with non-specific reactive change (ICC-reactive) (○). The enhancement in the arterial phase of ICC is correlated with AD ($P < 0.01$, $r = 0.509$). –, no or minimum enhancement; +, mild enhancement; and ++, strong enhancement. (B) The correlation between the arterial phase enhancement of intrahepatic cholangiocarcinoma (ICC) in magnetic resonance imaging (MRI) and microvessel density (MVD) in ICC with cirrhosis and precirrhotic liver (ICC-cirrhosis) (△) and with non-specific reactive change (ICC-reactive) (○). The enhancement in the arterial phase of ICC is correlated with MVD ($P < 0.01$, $r = 0.488$). –, no or minimum enhancement; +, mild enhancement; and ++, strong enhancement.

It was found in this study that using dynamic CT, almost all cases of ICC-cirrhosis showed strong contrast enhancement in the early phase, whereas about one-third of ICC-reactive showed strong enhancement, one-third showed mild enhancement and the remaining third showed no or minimum enhancement. Similarly in dynamic MRI, almost all cases of ICC-cirrhosis showed strong enhancement in the early phase, whereas about one-third of ICC-reactive showed strong enhancement, one-third showed mild enhancement and the remaining third showed no or minimum enhancement. These findings support the reports (3,8,16) that ICC in patients with chronic viral hepatitis or cirrhosis showed a hyperenhanced vascular pattern and also intense arterial uptake revealed by dynamic imaging, similar to HCC.

It was found that the arterial density in ICC-cirrhosis cases was higher than that in ICC-reactive cases and comparable to that in the CC component of HCC-ICC. The arterial density did not differ between ICC-cirrhosis and the cholangiocarcinoma component of HCC-ICC. Similarly, the microvessel density within tumours in ICC-cirrhosis cases was higher than that in ICC-reactive cases and comparable to that in CC component of HCC-ICC. The mean microvessel density in the cholangiocarcinoma components of HCC-ICC ended to be lower than that in ICC-cirrhosis. It is possible that the background lesion of ICC may be responsible at least partly for the dense arteries and microvessels in ICC-cirrhosis and cholangiocarcinoma components of HCC-ICC. In cirrhosis and precirrhotic liver, arterial branches are known to increase and small vasculatures including the peribiliary vascular plexus are also increased (9,23,24). It therefore seems plausible that ICC arising in cirrhosis and precirrhotic liver may maintain or retain such vasculatues characteristic of cirrhosis and precirrhotic liver after the malignant transformation of cholangiocytes. Alternatively, our previous study showed that phenotypes of ICC-cirrhosis were similar to those of cholangiocarcinoma components of HCC-ICC and different from ICC-reactive (9). Therefore, it is also possible that the tumour stroma of ICC-cirrhosis and the cholangiocarcinoma component of HCC-ICC share characteristics, such as increased density of arteries and microvessels, and such features are milder in ICC-reactive than in ICC-cirrhosis or the cholangiocarcinoma component of HCC-ICC. Further study of the difference in tumour stroma between ICC-cirrhosis and ICC-reactive is needed.

Arterial blood supply, venous drainage and other vascular characteristics play a crucial role in the diagnosis of liver tumours (25). Although the predominant radiological characteristic of ICC is hypovasculature, some cases show a contrast enhancement in the arterial phase identical to that in HCC, particularly for ICC in chronic viral hepatitis or cirrhosis (8,9,14,16,17). It was found in this study that in dynamic CT imaging, ICC cases with stronger enhancement showed higher arterial density and microvessel density, which were evaluated semiquantitatively. Dynamic MRI also showed a similar positive correlation between arterial density and microvessel density and early enhancement in ICCs. These results strongly support that hyperenhancement of ICC, especially in cirrhosis (8,16,17), may be because of increased densities of arteries and microvessels in the tumour. Such features were milder in ICC-reactive cases. The vasculature evaluated semiquantitatively may give a pathological basis for making a diagnosis of ICC or HCC in cirrhosis and precirrhotic liver, and studies on the mechanism of increased arterial density and microvessels are warranted. In addition, further study on the stroma of ICC including vasculature is mandatory to increase the differential diagnostic ability in imaging and also to evaluate the cholangiocarcinogenesis in cirrhosis and precirrhotic liver.

To assess the arterial density and microvessel density, we selected areas at random in the centre of the tumour. It may be possible to assess the invasive border of each tumour or the areas with the highest number of blood vessels ('hot spot' areas). In fact, the hot spot areas were evaluated in some studies, especially studies regarding angiogenetic factors, such as vascular endothelial growth factor (VEGF) and hypoxia-inducible factor-1α (HIF-1α) protein, whereas the random areas were evaluated in other studies. In the present study, we evaluated the areas selected at random in the centre of the tumour, because we would like to select the areas corresponding to the representative area in CT and MRI.

In conclusion, the vasculature in tumour stroma of ICC and the cholangiocarcinoma component of HCC-ICC increased in comparison with that of ICC-reactive. This may be the reason why ICC-cirrhosis showed enhanced contrast in the arterial phase during dynamic CT and MRI.

Acknowledgement

Conflict of interest: There is no conflict of interest regarding this manuscript.

Financial support: This study was supported in part by a Grant-in Aid for Scientific Research (B) from the Ministry of Education, Culture, Sports and Science and Technology of Japan (21590366).

References

1. Nakanuma Y, Curabo MP, Franceschi S, *et al.* A Intrahepatic cholangiocarcinoma. In: Bosman FT, Carneiro F, Hruban RH, Theise ND, eds. *WHO Classification of Tumours of the Digestive System; World Health Organization of Tumours*, 4th edn. Lyon: IARC, 2010; 217–24.
2. Okuda K, Nakanuma Y, Miyazaki M. Cholangiocarcinoma: recent progress. Part 1: epidemiology and etiology. *J Gastroenterol Hepatol* 2002; **17**: 1049–55.
3. Shaib YH, El-Serag HB, Nooka AK, *et al.* Risk factors for intrahepatic and extrahepatic cholangiocarcinoma: a hospital-based case-control study. *Am J Gastroenterol* 2007; **102**: 1016–21.
4. Nakanuma Y, Sato Y, Harada K, *et al.* Pathological classification of intrahepatic cholangiocarcinoma based on a new concept. *World J Hepatol* 2010; **2**: 419–27.
5. Nakanuma Y, Xu J, Harada K, *et al.* Pathological spectrum of intrahepatic cholangiocarcinoma arising in non-biliary, chronic advanced liver diseases. *Pathol Int* 2011; **61**: 298–305.
6. Tomimatsu M, Ishiguro N, Taniai M, *et al.* Hepatitis C virus antibody in patients with primary liver cancer (hepatocellular carcinoma, cholangiocarcinoma, and combined hepatocellular-cholangiocarcinoma) in Japan. *Cancer* 1993; **72**: 683–638.
7. Hai S, Kubo S, Yamamoto S, *et al.* Clinicopathologic characteristics of hepatitis C virus-associated intrahepatic cholangiocarcinoma. *Dig Surg* 2005; **22**: 432–9.

8. Vilana R, Forner A, Bianchi L, *et al.* Intrahepatic peripheral cholangiocarcinoma in cirrhosis patients may display a vascular pattern similar to hepatocellular carcinoma on contrast-enhanced ultrasound. *Hepatology* 2010; **51**: 2020–9.
9. Xu J, Sasaki M, Harada K, *et al.* Intrahepatic cholangiocarcinoma arising in chronic advanced liver disease and the cholangiocarcinomatous component of hepatocellular-cholangiocarcinoma share common phenotypes and cholangiocarcinogenesis. *Histopathology* 2011; **59**: 1090–9.
10. Kozaka K, Sasaki M, Fujii T, *et al.* A subgroup of intrahepatic cholangiocarcinoma with an infiltrating replacement growth pattern and a resemblance to reactive proliferating bile ductules: 'bile ductular carcinoma'. *Histopathology* 2007; **51**: 390–400.
11. Sasaki M, Tsuneyama K, Ishikawa A, Nakanuma Y. Intrahepatic cholangiocarcinoma in cirrhosis presents granulocyte and granulocyte-macrophage colony-stimulating factor. *Hum Pathol* 2003; **34**: 1337–44.
12. Nakanuma Y, Sasaki M, Ikeda H, *et al.* Pathology of peripheral intrahepatic cholangiocarcinoma with reference to tumorigenesis. *Hepatol Res* 2008; **38**: 325–34.
13. Okuda K, Nakanuma Y, Miyazaki M. Cholangiocarcinoma: recent progress. Part 2: molecular pathology and treatment. *J Gastroenterol Hepatol* 2002; **17**: 1056–63.
14. Chen LD, Xu HX, Xie XY, *et al.* Enhancement patterns of intrahepatic cholangiocarcinoma: comparison between contrast-enhanced ultrasound and contrast-enhanced CT. *Br J Radiol* 2008; **81**: 881–9.
15. Xu HX, Lu MD, Liu GJ, *et al.* Imaging of peripheral cholangiocarcinoma with low-mechanical index contrast-enhanced sonography and SonoVue: initial experience. *J Ultrasound Med* 2006; **25**: 23–33.
16. Nanashima A, Sumida Y, Abo T, *et al.* Relationship between pattern of tumor enhancement and clinicopathologic characteristics in intrahepatic cholangiocarcinoma. *J Surg Oncol* 2008; **9**: 535–9.
17. Rimola J, Forner A, Reig M, *et al.* Cholangiocarcinoma in cirrhosis: absence of contrast washout in delayed phases by magnetic resonance imaging avoids misdiagnosis of hepatocellular carcinoma. *Hepatology* 2009; **50**: 791–8.
18. Nakamura K, Zen Y, Sato Y, *et al.* Vascular endothelial growth factor, its receptor Flk-1, and hypoxia inducible factor-1alpha are involved in malignant transformation in dysplastic nodules of the liver. *Hum Pathol* 2007; **38**: 1532–46.
19. Pugacheva O, Matsui O, Kozaka K, *et al.* Detection of small hypervascular hepatocellular carcinomas by EASL criteria: comparison with double-phase CT during hepatic arteriography. *Eur J Radiol* 2011; **80**: e201–6.
20. Hattori Y, Gabata T, Zen Y, *et al.* Poorly enhanced areas of pancreatic adenocarcinomas on late-phase dynamic computed tomography: comparison with pathological findings. *Pancreas* 2010; **39**: 1263–70.
21. Celli N, Gaiani S, Piscaglia F, *et al.* Characterization of liver lesions by real-time contrast-enhanced ultrasonography. *Eur J Gastroenterol Hepatol* 2007; **19**: 3–14.
22. Xu HX, Lu MD, Liu GJ, *et al.* Imaging of peripheral cholangiocarcinoma with low-mechanical index contrast-enhanced sonography and SonoVue: initial experience. *J Ultrasound Med* 2006; **25**: 23–33.
23. Sato S, Ohnishi K, Sugita S, Okuda K. Splenic artery and superior mesenteric artery blood flow: nonsurgical Doppler US measurement in healthy subjects and patients with chronic liver disease. *Radiology* 1987; **164**: 347–52.
24. Kobayashi S, Nakanuma Y, Matsui O. Intrahepatic peribiliary vascular plexus in various hepatobiliary diseases: a histological survey. *Hum Pathol* 1994; **25**: 940–6.
25. Okuda K. *Hepatobiliary Diseases. Pathophyisology and Imaging*. Oxford: Blackwell Science, 2001.

HEPATOLOGY
Official Journal of the American Association for the Study of Liver Diseases

Significance of Immunoglobulin G4 (IgG4)-Positive Cells in Extrahepatic Cholangiocarcinoma: Molecular Mechanism of IgG4 Reaction in Cancer Tissue

Kenichi Harada,[1] Shinji Shimoda,[2] Yasushi Kimura,[1] Yasunori Sato,[1] Hiroko Ikeda,[3] Saya Igarashi,[1] Xiang-Shan Ren,[1] Hirohide Sato,[1] and Yasuni Nakanuma[1]

IgG4 reactions consisting of marked infiltration by immunoglobulin G4 (IgG4)-positive plasma cells in affected organs is found in cancer patients as well as patients with IgG4-related diseases. Notably, extrahepatic cholangiocarcinomas accompanying marked IgG4 reactions clinicopathologically mimic IgG4-related sclerosing cholangitis. The regulatory cytokine interleukin (IL)-10 is thought to induce the differentiation of IgG4-positive cells. In this study, to clarify the mechanism of the IgG4 reaction in extrahepatic cholangiocarcinoma, we investigated nonprofessional antigen-presenting cells (APCs) generating IL-10–producing regulatory T cells (anergy T cells) and Foxp3-positive regulatory cells producing IL-10. Immunohistochemistry targeting IgG4, HLA-DR, CD80, CD86, and Foxp3 was performed using 54 cholangiocarcinoma specimens from 24 patients with gallbladder cancer, 22 patients with common bile duct cancer, and eight patients with cancer of the Papilla of Vater. Moreover, a molecular analysis of Foxp3 and IL-10 was performed using a cultured human cholangiocarcinoma cell line. Consequently, 43% of the cholangiocarcinomas were found to be abundant in IgG4. Those expressing HLA-DR but lacking costimulatory molecules (CD80 and CD86) and those expressing Foxp3 detected by an antibody recognizing the N terminus accounted for 54% and 39% of cases, respectively. Moreover, the number of IgG4-positive cells was larger in these cases than in other groups. In cultured cells, the presence of a splicing variant of Foxp3 messenger RNA and the expression of IL-10 were demonstrated. *Conclusion*: Extrahepatic cholangiocarcinoma is often accompanied by significant infiltration of IgG4-positive cells. Cholangiocarcinoma cells could play the role of nonprofessional APCs and Foxp3-positive regulatory cells, inducing IgG4 reactions via the production of IL-10 indirectly and directly, respectively. (HEPATOLOGY 2012;56:157-164)

Biliary tract cancers can be anatomically divided into intrahepatic and extrahepatic cholangiocarcinomas, the latter including hepatic hilar cancer, common bile duct cancer, gallbladder cancer, and cancer of the Papilla of Vater. The biological behavior and carcinogenesis of each cancer differ, but the histology of most biliary tract cancers is the same as that of ordinary adenocarcinomas. In addition to neoplastic lesions, several types of cholangitis causing biliary stenosis are important in the differential diagnosis of biliary diseases. Particularly, primary sclerosing cholangitis and a complication of immunoglobulin G4 (IgG4)-related systemic diseases, IgG4-related sclerosing cholangitis, clinicopathologically mimic extrahepatic cholangiocarcinomas.

IgG4 is a minor immunoglobulin subtype composing 3%-6% of all the IgG circulating in adults,[1] but is important for a systemic disorder, IgG4-related disease, that features elevated serum IgG4 levels and abundant

Abbreviations: APC, antigen-presenting cell; DC, dendritic cell; ELISA, enzyme-linked immunosorbent assay; HPF, high-power field; IgG4, immunoglobulin G4; IL, interleukin; MHC-II, major histocompatibility complex class II; mRNA, messenger RNA; PCR, polymerase chain reaction; RT-PCR, reverse-transcription polymerase chain reaction; Treg, regulatory T cell.

From the [1]Department of Human Pathology, Kanazawa University Graduate School of Medicine, Kanazawa, Japan; [2]Medicine and Biosystemic Science, Kyushu University Graduate School of Medical Sciences, Fukuoka, Japan; and the [3]Division of Pathology, Kanazawa University Hospital, Kanazawa, Japan.

Received November 6, 2011; accepted January 19, 2012.

Supported by grant no.23590393 from the Ministry of Education, Culture, Sports, Science and Technology of Japan (to K.H.) and Health and Labour Sciences Research Grants for Research on Measures for Intractable Diseases.

Address reprint requests to: Kenichi Harada, M.D., Department of Human Pathology, Kanazawa University Graduate School of Medicine, Kanazawa 920-8640, Japan. E-mail: kenichih@med.kanazawa-u.ac.jp; fax: (81)-76-234-4229.

View this article online at wileyonlinelibrary.com.

DOI 10.1002/hep.25627

Potential conflict of interest: Nothing to report.

infiltration with IgG4-positive plasma cells in affected organs.[1-3] Moreover, IgG4-related cholangitis and pancreatitis (autoimmune pancreatitis, type 1) are characterized by sclerosing lesions (storiform fibrosis) and cholangiocarcinomas and pancreatic cancer usually accompany some degree of desmoplastic change and also, in some cases of pancreatic cancer, IgG4 reactions.[4] Therefore, a pathological examination is necessary to differentiate IgG4-related diseases from tumors in pancreaticobiliary lesions. We have already observed that extrahepatic cholangiocarcinomas also accompany various degrees of IgG4 reactions assumed to be associated with the evasion of immunosurveillance (Kimura et al., unpublished data). However, the mechanisms inducing IgG4 reactions in cholangiocarcinoma tissue are still unknown.

Interleukin (IL)-10, a regulatory cytokine mainly produced by Foxp3+ regulatory T cells (Treg cells), T helper 2 cells, and IL-10–producing Treg cells, is thought to induce the differentiation of IgG4-positive plasma cells or favor B cell switching to IgG4 in the presence of IL-4.[5,6] The expression of Foxp3 and IL-10 has been demonstrated in several carcinoma tissues and cultured cancer cell lines, suggesting that cancer cells themselves induce the Treg cell–like immunoregulatory milieu to evade immunosurveillance.[7-10].

Major histocompatibility complex class II (MHC-II)–positive cells lacking the costimulatory molecules CD80 (B7-1) and CD86 (B7-2) induce anergy to native T cells. Among T cell subsets, Treg type 1 cells characterized by the production of IL-10 are induced by immature dendritic cells (DCs).[11] Moreover, costimulation-dependent T cell clones stimulated without provision of the costimulatory signal were demonstrated not to be proliferative, but to differentiate into IL-10–producing anergic T cells in primary biliary cirrhosis.[12] In addition to immunocompetent cells such as DCs, nonimmunocompetent cells, including carcinoma and normal epithelial cells, have been demonstrated to express MHC-II, indicating an ability for antigen presentation, but these MHC-II–positive epithelial cells are usually called nonprofessional antigen-presenting cells (APCs), differing from professional APCs such as DCs. Several studies have suggested that antigen presentation by MHC-II–positive epithelial cells that lack costimulation signals, such as keratinocytes and pancreatic islet cells, would favor the generation of anergic T cells.[13-15]

It is clinicopathologically important, but practically difficult, to differentiate between IgG4-related sclerosing cholangitis and extrahepatic cholangiocarcinoma. In this study, we retrospectively evaluated IgG4-positive plasma cells in extrahepatic cholangiocarcinomas and mechanisms in terms of cholangiocarcinoma cells as nonprofessional APCs and regulatory cells. This study should help to clarify the pathological significance of IgG4 reactions in cholangiocarcinomas and also IgG4-related diseases.

Patients and Methods

Patients and Tissue Preparations. Formalin-fixed and paraffin-embedded sections of 54 surgically resected specimens from 24 gallbladder cancers, 22 common bile duct cancers, and eight cancers of the Papilla of Vater (29 men, 25 women; average age, 74 years) were obtained from the registry of liver diseases in the Department of Pathology, Kanazawa University School of Medicine. Each cholangiocarcinoma was classified histologically as a well-differentiated (including papillary), moderately differentiated, or poorly differentiated adenocarcinoma based on the predominant histological grade. Special histological types such as adenosquamous carcinoma and mucinous carcinoma were not included in the present study. Serial sections (4 μm) were prepared from each formalin-fixed, paraffin-embedded block.

Immunohistochemistry. The deparaffinized and rehydrated sections were microwaved in citrate buffer (pH 6.0) for CD80 and CD86 or ethylene diamine tetraacetic acid buffer (pH 9.0) for Foxp3 for 20 minutes in a microwave oven. Following the blocking of endogenous peroxidase activity, these sections were incubated at 4°C overnight with antibodies against IgG4 (mouse monoclonal; diluted 1:200; Southern Biotech, Birmingham, AL), Foxp3 that reacts with the C terminus (mouse monoclonal; 5 μg/mL; Abcam, Tokyo, Japan), Foxp3 that reacts with the N terminus (rat monoclonal, 2.5 μg/mL, eBioscience, San Diego, CA), HLA-DR (mouse monoclonal, 0.5 μg/mL, Dako Japan, Tokyo), CD80 (rabbit monoclonal, 1:200, Epitomics, Burlingame, CA), and CD86 (rabbit monoclonal, 1:250, Abcam, Tokyo, Japan) and then at room temperature for 1 hour with anti-mouse, anti-rabbit, or anti-goat immunoglobulin conjugated to a peroxidase-labeled dextran polymer (Simple Staining Kit; Nichirei, Tokyo, Japan). After a benzidine reaction, sections were counterstained lightly with hematoxylin. No positive staining was obtained when the primary antibodies were replaced with an isotype-matched, nonimmunized immunoglobulin as a negative control of the staining procedures.

Histological Examination. In addition to the histological observations by hematoxylin and eosin staining, the distribution of the immunopositive cells was

examined. In a primary survey, we examined all tumorous areas in each specimen and, for counting IgG4-positive mononuclear cells, selected three representative areas containing IgG4-positive plasma cells, and expressed the results as the mean number of immunopositive cells in high-power fields (HPFs). Because ≥10 IgG4-positive cells/HPF is proposed according to HISORt (Histology, Imaging, Serology, Other organ involvement, Response to therapy) criteria published for autoimmune pancreatitis,[16,17] the cases with ≥10 and <10 IgG4-positive cells/HPF on average were evaluated as IgG4-rich and IgG4-poor cases, respectively. For the expression of Foxp3, HLA-DR, CD80, and CD86, positive carcinoma cells were evaluated as positive (distinct expression) or negative (no or faint expression) according to the staining intensity.

Cultured Cells. Two commercially available cell lines, HuCCTl and MCF7 (positive control of IL-10),[10] were obtained from Health Science Research Resources Bank (Osaka, Japan). The cell lines were derived from cholangiocarcinoma and breast cancer cells, respectively.

Reverse-Transcription Polymerase Chain Reaction. The cell lines were cultured in flasks with a standard medium for 48 hours. Cultured cells were collected from the flasks or plates with a cell scraper for determination of the baseline messenger RNA (mRNA) expression of Foxp3 and IL-10 by via reverse-transcription polymerase chain reaction (RT-PCR). Lymph node tissue was also used as a positive control for Foxp3 mRNA. Briefly, total RNA was isolated from each sample with the RNeasy Total RNA System (QIAGEN, Hilden, Germany) and treated with RNase-Free DNaseI. For RT-PCR, 1 μg of total RNA, M-MLV RTase (ReverTra Ace, Toyobo, Tokyo, Japan) and oligo-dT primers were used. Polymerase chain reaction (PCR) amplification was performed using DNA polymerase (Takara EX Taq, Takara, Tokyo, Japan) and specific primers for human mRNA sequences (Table 1). The glyceraldehyde 3-phosphate dehydrogenase mRNA was used as a housekeeping gene. Following After PCR, an annealing of primers for 1 minute, and an extension at 72°C for 2 minutes (the annealing temperature and cycle number are shown in Table 1), PCR products were subjected to agarose gel electrophoresis.

Enzyme-Linked Immunosorbent Assay. Approximately 1×10^4 HuCCT1 cells per well in 96-well plates were cultured for 24 hours. Supernatants were then tested for human IL-10 via enzyme-linked immunosorbent assay (ELISA) (R&D Systems).

Statistical Analysis. Data were analyzed using the Welch t test; $P < 0.05$ was considered statistically significant.

Table 1. Primers Used for RT-PCR

Transcript	Primers	Product Size
Foxp3		
Exon 1	Forward: 5′-ACCGTACAGCGTGGTTTTTC-3′	111 bp
	Reverse: 5′-AGGCTTGGTGAAGTGGACTG-3′	
Exon 3	Forward: 5′-TGCCTCCTCTTCTTCCTTGA-3′	125 bp
	Reverse: 5′-GGAGGAGTGCCTGTAAGTGG-3′	
Exons 10-12	Forward: 5′- CACAACATGCGACCCCCTTTCACC -3′	167 bp
	Reverse: 5′- AGGTTGTGGCGGATGGCGTTCTTC-3′	
Exon 12	Forward: 5′- CAGCTGCTCGCACAGATTAC -3′	91 bp
	Reverse: 5′- TTGGGGTTTGTGTTGAGTGA-3′	
IL-10	Forward: 5′- TGCAAAACCAAACCACAAGA -3′	325 bp
	Reverse: 5′- GCATCACCTCCTCCAGGTAA-3′	
GAPDH	Forward: 5′-GCACCGTCAAGGCTGAGAAC-3′	142 bp
	Reverse: 5′-ATGGTGGTGAAGACGCCAGT-3′	

Abbreviations: bp, base pairs; GAPDH, glyceraldehyde 3-phosphate dehydrogenase; IL-10, interleukin 10; RT-PCR, reverse-transcription polymerase chain reaction.

Results

Infiltration of IgG4-Positive Cells in Extrahepatic Cholangiocarcinoma. Immunohistochemistry revealed that IgG4-positive plasma cells were scattered within and around cancerous nests to various degrees in most cases (Fig. 1). In the cases with marked infiltration, the IgG4-positive cells were prominent with intermingling of other inflammatory cells. Figure 1C shows the number of IgG4-positive cells/HPF in extrahepatic cholangiocarcinomas from common bile ducts, gallbladder, and the Papilla of Vater, but there was no significant difference in IgG4-positive cell counts among anatomical locations of extrahepatic cholangiocarcinomas. Therefore, they were integrated as shown in Fig. 1D. Consequently, the combined quantitative evaluation revealed that 23 (43%) of 54 cholangiocarcinoma patients had ≥10 IgG4-positive cells/HPF. There was no correlation between the density of IgG4-positive cells and any clinicopathological factor including age, sex, anatomical location (common bile ducts, gallbladder, and the Papilla of Vater), or the histological differentiation (well, moderate, and poor) of extrahepatic cholangiocarcinoma.

Cholangiocarcinoma Cells as Nonprofessional APCs and Their Association with IgG4 Reactions. Representative images of immunostaining are shown in Fig. 2. Expression of HLA-DR was found in some infiltrating immunocompetent cells. Moreover, HLA-DR–positive cholangiocarcinoma cells were also found in 33 of 54 cases. HLA-DR expression in tumor cells showed uniformity and metastatic foci in lymph nodes as well as main tumors expressing HLA-DR. In contrast, the expression of costimulatory molecules (CD80 and CD86) was mostly faint or absent. Only four cases were clearly positive for CD86 in cholangiocarcinoma

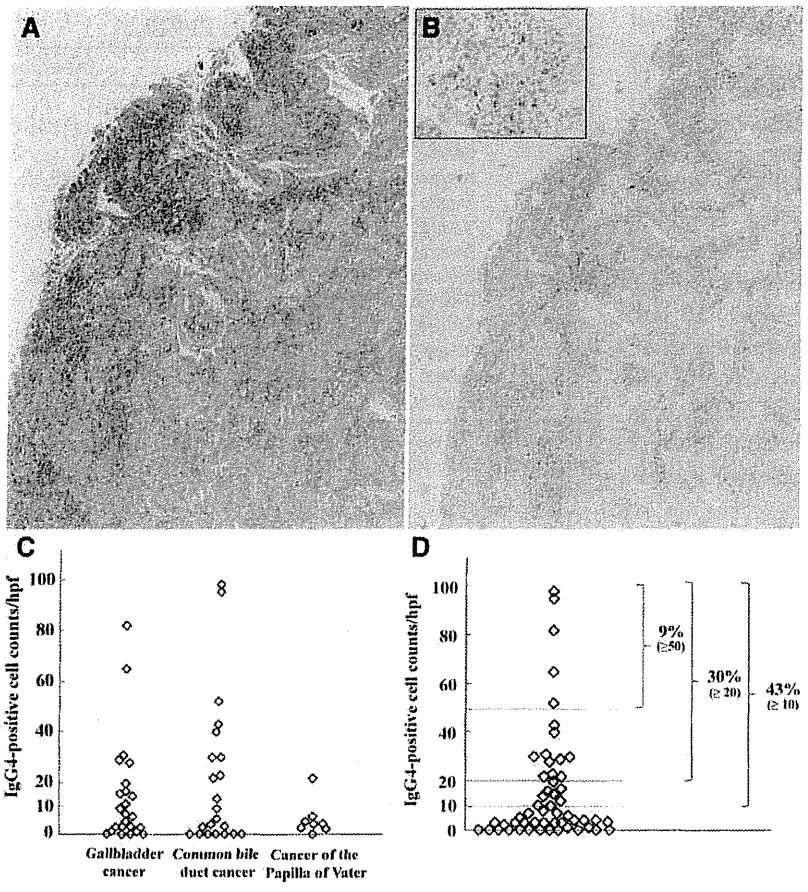

Fig. 1. IgG4-positive cells in extrahepatic cholangiocarcinomas. (A) Gallbladder cancer. A papillary adenocarcinoma with prominent inflammatory cells was found (original magnification: ×40). (B) Immunohistochemistry for IgG4. Numerous IgG4-posituve cells are present in the inflamed stroma (original magnification: ×40). The inset shows a higher magnification (original magnification: ×400). (C) Number of IgG4-positive cells/HPF in common bile duct cancer, gallbladder cancer, and cancer of the Papilla of Vater. There was no significant difference in IgG4-positive cell counts among anatomical locations of extrahepatic cholangiocarcinoma. (D) Number of IgG4-positive cells in cholangiocarcinoma. A quantitative evaluation revealed that 23 (43%), 16 (30%), and five (9%) of 54 cholangiocarcinoma patients had ≥10, ≥20, and ≥50 IgG4+ cells/HPF, respectively.

cells, and all of them were positive for HLA-DR. No cases evidently expressed CD80. Cholangiocarcinoma cells expressing HLA-DR but lacking costimulatory molecules (CD80 and CD86) were found in 29 of 54 cases (54%) and suggested to act as nonprofessional APCs inducing IL-10–producing anergy T cells. The relation between IgG4 reactions and HLA-DR and costimulatory molecules in cancer cells is shown in Fig. 3. In cases of positivity for HLA-DR and negativity for costimulatory molecules, the number of IgG4-positive cells was significantly higher than in cases of negativity for HLA-DR and of positivity for both HLA-DR and costimulatory molecules.

Cholangiocarcinoma Cells as Regulatory Cells. Immunohistochemistry using the antibody reacting with the C terminus of Foxp3 detected only mononuclear cells (Treg cells), but the antibody reacting with the N terminus highlighted cholangiocarcinoma cells as well as Treg cells (Fig. 4A). The cytoplasm as well as nucleus of tumor cells was positive in several cases. However, because Foxp3 is a transcription factor, the nuclear pattern was evaluated as functional expression. Consequently, 21 of 54 (39%) cholangiocarcinomas tested positive for Foxp3 by the antibody reacting with the N terminus. The relation between the IgG4 reaction and Foxp3 expression in cholangiocarcinoma cells is shown in Fig. 5. In cases of positivity for Fopx3, the number of IgG4-positive cells was significantly higher than in cases of negativity for Foxp3.

RT-PCR analysis demonstrated that a cholangiocarcinoma cell line, HuCCT1, expressed the mRNA of Foxp3, but close examination using four sets of primers corresponding to exons 1, 3, 10-12, and 12 revealed a lack of exon 3 (Fig. 6), suggesting the presence of a splicing variant of Foxp3 in cholangiocarcinoma cells. Moreover, RT-PCR and ELISA revealed that HuCCT1 cells expressed IL-10 mRNA (Fig. 6) and protein in the culture medium at 7.8-15.6 pg/mL.

Discussion

IgG4 is important to the pathogenesis of IgG4-related diseases. However, patients with pancreatic adenocarcinomas accompanying IgG4 reactions and/or

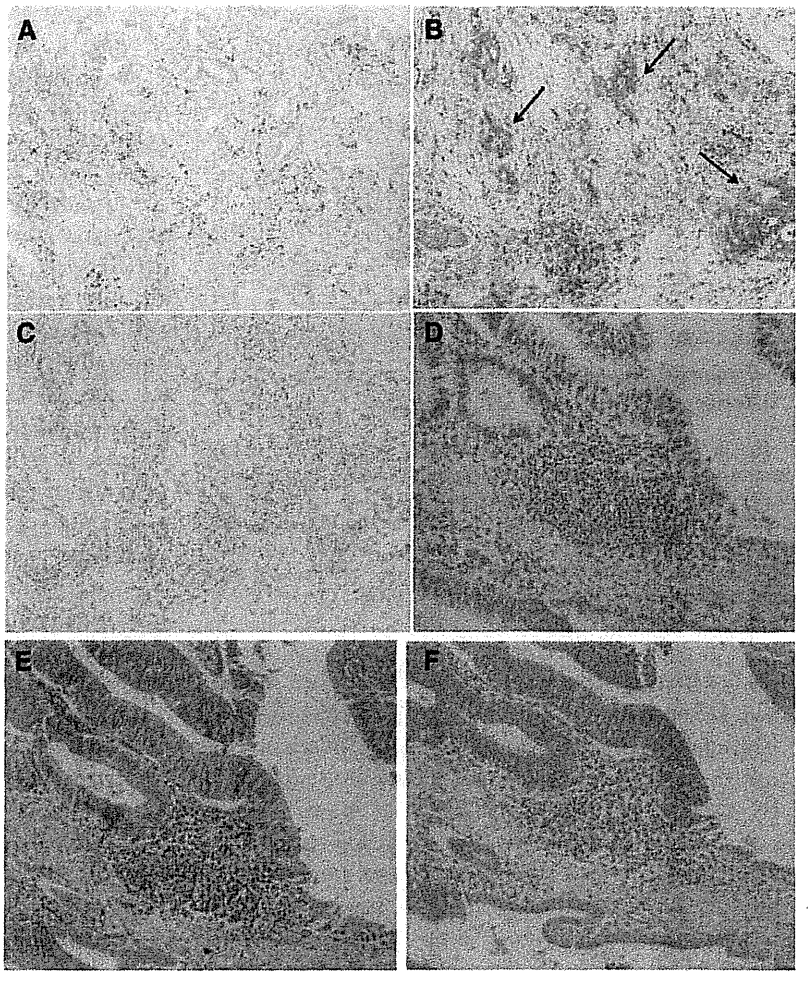

Fig. 2. Immunohistochemistry for IgG4 (A,D), HLA-DR (B,E), CD80 (C), and CD86 (F). (A-C) IgG4-rich case of gallbladder cancer. Numerous IgG4-positive cells were found within cancer tissue (A). In addition to infiltrating mononuclear cells, carcinoma cells also tested positive for HLA-DR (B, arrows). No tumor cells were positive for CD80 (C). (D-F) IgG4-poor case of common bile duct cancer. No IgG4-positive cells were found (D), but obvious expression of HLA-DR and CD86 in carcinoma cells was found (E,F). Original magnification: ×200.

elevated serum IgG4 levels[4,18-20] and with pancreatic and biliary cancers arising from IgG4-related diseases[20-22] have been reported, though a cause-and-effect relationship between IgG4 reactions and cancers has yet to be demonstrated. Moreover, in IgG4-nonrelated diseases, including primary sclerosing cholangitis, IgG4 reactions were found to various degrees.[23,24] Therefore, the presence of IgG4-positive cells is not a histological hallmark of IgG4-related diseases, and IgG4 reactions are speculated to be nonspecific in several pathological conditions, including cholangiocarcinomas. The present study also demonstrated the presence of extrahepatic cholangiocarcinoma cases with abundant IgG4 reaction, though there was no significant difference in IgG4-positive cell counts among anatomical locations of extrahepatic cholangiocarcinomas (common bile ducts, gallbladder, and the Papilla of Vater). The significance and mechanisms of IgG4 reactions in cancers as well as IgG4-related diseases are still unknown, but we speculated that cancer cells directly participate in the histogenesis of IgG4 reactions. Because the regulatory cytokine IL-10 is known to induce the differentiation of IgG4-positive plasma cells or favor B cell switching to IgG4 in the presence of IL-4,[5,6] we noted the IL-10–related regulatory cytokine network around cholangiocarcinoma tissue in this study.

Immunohistochemistry for MHC-II (HLA-DR) and costimulatory molecules (CD80 and CD86) revealed that cholangiocarcinoma cells as well as professional APCs such as B cells and DCs expressed HLA-DR and CD86. The expression of CD80 was limited in some APCs and not found in cholangiocarcinoma cells. Consequently, cholangiocarcinoma cells expressing HLA-DR, but lacking costimulatory molecules (CD80 and CD86) were found in 54% of cases. These cancer cells could act as nonprofessional APCs, possibly generating IL-10–producing Treg cells (anergy T cells), and then an IL-10–predominant cytokine milieu could cause the induction of IgG4-positive cells.[5,6] In these phenotypic cases, the number of IgG4-positive

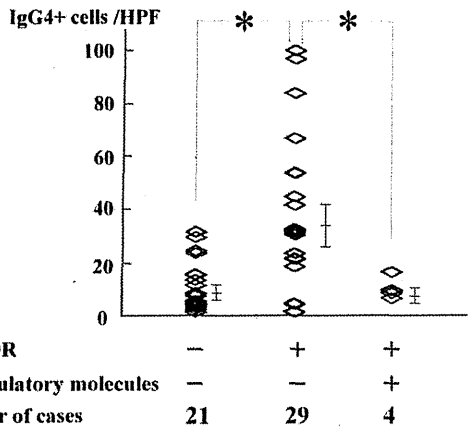

Fig. 3. Correlation between IgG4-positive cell counts and antigen-presenting-related molecules in cholangiocarcinoma. The number of IgG4-positive cells in the cholangiocarcinoma cases expressing HLA-DR but lacking costimulatory molecules (CD80 and CD86) is significantly higher than those of negativity for HLA-DR and costimulatory molecules and of positivity for both HLA-DR and costimulatory molecules. Bars indicate the mean ± SEM. *$P < 0.05$.

cells infiltrating carcinoma tissue was higher than in HLA-DR–negative cases and both HLA-DR– and CD86-positive cases, confirming this speculation. Cells positive for both HLA-DR and CD86 are suggested to play the role of professional APCs, as it was reported that MHC-II–positive thyroid epithelial cells could present antigens to T cells and activate autoreactive T cells.[25,26] Although further study is needed to clarify the functional mechanism of these cholangiocarcinoma cells as APCs, this study demonstrated that HLA-DR– and CD86-positive cancer cells were not associated with IgG4 reactions in cholangiocarcinoma tissue.

As to pathogenesis of IgG4 reactions in IgG4-related diseases, the participation of $CD4^+CD25^+Foxp3^+$ Treg cells, which are capable of producing IL-10, has been speculated.[27] Foxp3 is thought to be the master transcription factor of Treg cells and, until recently, Foxp3 expression was thought to be restricted to the T cell lineage. However, immunohistochemistry and flow cytometric analysis demonstrated that some carcinoma tissues and cultured cancer cell lines expressed Foxp3.[7-10] Immunohistochemistry using the antibody recognizing the N terminus, but not the C terminus, of Foxp3-highlighted cholangiocarcinoma tissue in 39% of cases as well as Treg cell morphology, suggesting the presence of the splicing variant of Foxp3 in cholangiocarcinoma cells. Molecular analysis using a cholangiocarcinoma cell line demonstrated that the cells expressed mRNA of Foxp3, but lack Exon 3. This type of splicing variant has already been reported in a melanoma cell line and created a novel amino acid caused by a frame shift at the C terminus.[9] This is why the antibody recognizing the C terminus of Foxp3 could not detect the variant of Foxp3 found in cholangiocarcinoma tissue. Although a functional analysis of this variant as a transcription factor is necessary, it has already been reported that Foxp3 expression is closely correlated with the expression of IL-10 in all Foxp3-positive cell lines.[10] The present study, using a cholangiocarcinoma cell line, also demonstrated that cells express mRNA of IL-10 as well as Foxp3.

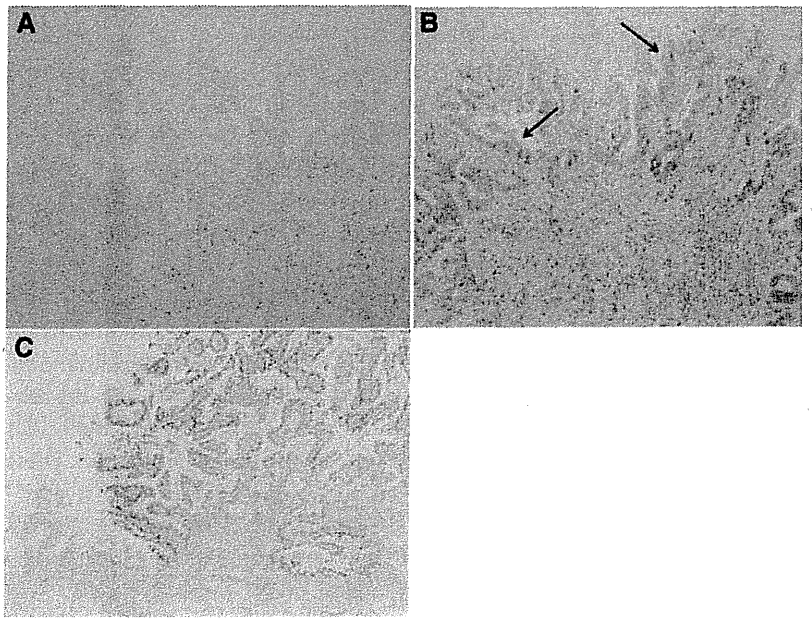

Fig. 4. Foxp3 expression in cholangiocarcinoma. Immunohistochemistry using the antibody recognizing the C terminus (A) and N terminus (B,C) of Foxp3. The antibody reacting with the C terminus detects only mononuclear cells (Treg cells) in the nuclear pattern (A). In contrast, the antibody reacting with the N terminus highlights the nucleus and cytoplasm of cholangiocarcinoma cells as well as Treg cells (B, arrows), but the localized expression in the nucleus is also found in cholangiocarcinoma cells (C). Original magnification for panels A and B is ×100; magnification for panel C is ×40.

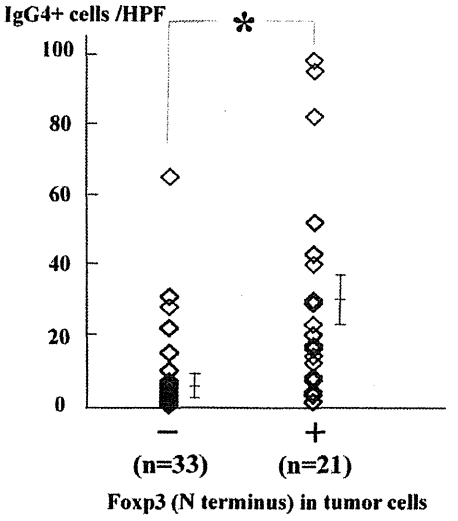

Fig. 5. Correlation between IgG4-positive cell counts and Foxp3 expression in cholangiocarcinoma. Nuclear expression of Foxp3 is found in 21 cases of cholangiocarcinoma and in these cases, the number of IgG4-positive cells was significantly higher than those of negativity for Foxp3. Bars indicate the mean ± S.E.M. $*P < 0.05$.

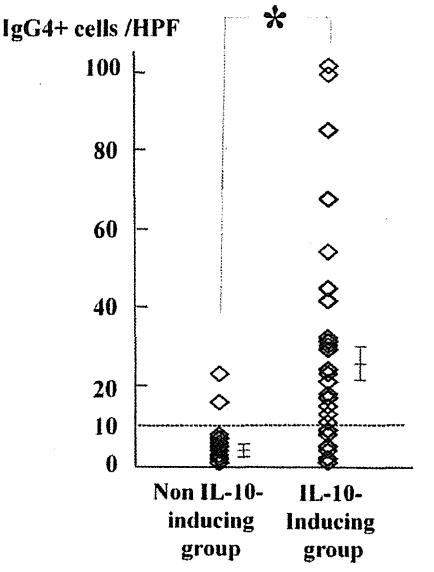

Fig. 7. Correlation between IgG4-positive cell counts and IL-10-predominant milieu. All cases were divided into two categories. The non-IL-10-inducing group includes MHC-II (HLA-DR)-negative and Foxp3-negative cases and MHC-II-positive, costimulatory molecule (CD86)-positive, and Foxp3-negative cases. The IL-10-inducing group includes MHC-II-positive and costimulatory molecule-negative cases and Foxp3-positive cases. All but two cases in the non-IL-10-inducing group were <10 IgG4+ cells/HPF, and the number of IgG4-positive cells in the IL-10-inducing group was significantly higher than that of the non-IL-10-inducing group. Bars indicate the mean ± SEM. $*P < 0.05$.

Moreover, the IL-10 protein was detected in the culture medium by ELISA at a concentration of 7.8-15.6 pg/mL, suggesting that the production of IL-10 was preserved with this splicing variant. This finding suggests that cholangiocarcinoma cells themselves function in immunosuppression similar to Treg cells via IL-10 production. This was supported by the present data that in Foxp3-positive cases, the number of IgG4-positive cells infiltrating cholangiocarcinoma tissues was higher than that in Foxp3-negative cases, though several negative cases still accompanied a significant IgG4 reaction (≥10 IgG4+ cells/HPF).

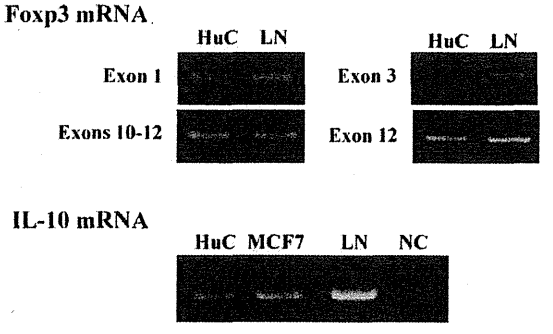

Fig. 6. Detection of Foxp3 and IL-10 mRNAs in the cultured cholangiocarcinoma cell line HuCCT1 (HuC). RT-PCR analysis using four sets of primers corresponding to exons 1, 3, 10-12, and 12 demonstrated that HuC expressed the mRNA of Foxp3, but lacked exon 3. Moreover, HuC expressed IL-10 mRNA. Each RT-PCR product yielded bands of the appropriate molecular weight. MCF7 (breast cancer cell line) and lymph node (LN) were used as positive controls, and negative control (NC) was obtained by omitting reverse transcriptase for reverse transcription of HuC.

In this study, we demonstrated two different types of IgG4 reactions in cholangiocarcinoma tissues. Although statistical significance could be obtained in terms of cholangiocarcinoma as both nonprofessional APCs and IL-10–producing regulatory cells, some cases deviated from each mechanism. Therefore, as shown in Fig. 7, we divided all cases into a non–IL-10–inducing group and an IL-10–inducing group and re-evaluated the present results accordingly. The former (n = 24) consisted of MHC-II–negative and Foxp3-negative cases and MHC-II–positive, costimulatory molecule (CD86)-positive, and Foxp3-negative cases; the latter (n = 30) included MHC-II–positive, costimulatory molecule–negative, and Foxp3-positive cases. This combined analysis demonstrated that all but two cases in the non–IL-10–inducing group were poor in IgG4 (<10 IgG4+ cells/HPF) and that the difference in IgG4 reactions between the IL-10–inducing group and the non–IL-10–inducing group was significant compared with that of the individual analysis in terms of nonprofessional APCs and IL-10–producing

regulatory cells. This finding indicates that cholangiocarcinoma cells directly participate in the induction of IgG4 reactions via an IL-10–predominent cytokine milieu as nonprofessional APCs and/or regulatory cells. However, the presence of IgG4-rich cases belonging to the non–IL-10–inducing group suggests another possible mechanism inducing IgG4 reactions in cholangiocarcinomas. Further studies are needed to clarify the mechanism of IgG4 reactions.

In conclusion, the marked infiltration of IgG-positive cells is found in several cases of cholangiocarcinoma, indicating that we should consider the differentiation of IgG4-related diseases and cholangiocarcinoma. The IgG4 reactions in cholangiocarcinomas, moreover, are closely associated with the IL-10–predominant regulatory cytokine milieu caused by cancer cells themselves directly and indirectly. Because IL-10 plays a primary role in suppressing immune responses, IgG4 reactions in cholangiocarcinoma might reflect evasion from immunosurveillance.

References

1. Hamano H, Kawa S, Horiuchi A, Unno H, Furuya N, Akamatsu T, et al. High serum IgG4 concentrations in patients with sclerosing pancreatitis. N Engl J Med 2001;344:732-738.
2. Hamano H, Kawa S, Ochi Y, Unno H, Shiba N, Wajiki M, et al. Hydronephrosis associated with retroperitoneal fibrosis and sclerosing pancreatitis. Lancet 2002;359:1403-1404.
3. Zen Y, Nakanuma Y. IgG4-related disease: a cross-sectional study of 114 cases. Am J Surg Pathol 2010;34:1812-1819.
4. Dhall D, Suriawinata AA, Tang LH, Shia J, Klimstra DS. Use of immunohistochemistry for IgG4 in the distinction of autoimmune pancreatitis from peritumoral pancreatitis. Hum Pathol 2010;41:643-652.
5. Robinson DS, Larche M, Durham SR. Tregs and allergic disease. J Clin Invest 2004;114:1389-1397.
6. Jeannin P, Lecoanet S, Delneste Y, Gauchat JF, Bonnefoy JY. IgE versus IgG4 production can be differentially regulated by IL-10. J Immunol 1998;160:3555-3561.
7. Hinz S, Pagerols-Raluy L, Oberg HH, Ammerpohl O, Grussel S, Sipos B, et al. Foxp3 expression in pancreatic carcinoma cells as a novel mechanism of immune evasion in cancer. Cancer Res 2007;67:8344-8350.
8. Wang WH, Jiang CL, Yan W, Zhang YH, Yang JT, Zhang C, et al. FOXP3 expression and clinical characteristics of hepatocellular carcinoma. World J Gastroenterol 2010;16:5502-5509.
9. Ebert LM, Tan BS, Browning J, Svobodova S, Russell SE, Kirkpatrick N, et al. The regulatory T cell-associated transcription factor FoxP3 is expressed by tumor cells. Cancer Res 2008;68:3001-3009.
10. Karanikas V, Speletas M, Zamanakou M, Kalala F, Loules G, Kerenidi T, et al. Foxp3 expression in human cancer cells. J Transl Med 2008;6:19.
11. Battaglia M, Gianfrani C, Gregori S, Roncarolo MG. IL-10-producing T regulatory type 1 cells and oral tolerance. Ann N Y Acad Sci 2004; 1029:142-153.
12. Shimoda S, Ishikawa F, Kamihira T, Komori A, Niiro H, Baba E, et al. Autoreactive T-cell responses in primary biliary cirrhosis are proinflammatory whereas those of controls are regulatory. Gastroenterology 2006;131:606-618.
13. Bal V, McIndoe A, Denton G, Hudson D, Lombardi G, Lamb J, et al. Antigen presentation by keratinocytes induces tolerance in human T cells. Eur J Immunol 1990;20:1893-1897.
14. Markmann J, Lo D, Naji A, Palmiter RD, Brinster RL, Heber-Katz E. Antigen presenting function of class II MHC expressing pancreatic beta cells. Nature 1988;336:476-479.
15. Lombardi G, Arnold K, Uren J, Marelli-Berg F, Hargreaves R, Imami N, et al. Antigen presentation by interferon-gamma-treated thyroid follicular cells inhibits interleukin-2 (IL-2) and supports IL-4 production by B7-dependent human T cells. Eur J Immunol 1997;27:62-71.
16. Ghazale A, Chari ST, Zhang L, Smyrk TC, Takahashi N, Levy MJ, et al. Immunoglobulin G4-associated cholangitis: clinical profile and response to therapy. Gastroenterology 2008;134:706-715.
17. Chari ST, Smyrk TC, Levy MJ, Topazian MD, Takahashi N, Zhang L, et al. Diagnosis of autoimmune pancreatitis: the Mayo Clinic experience. Clin Gastroenterol Hepatol 2006;4:1010-1016; quiz 1934.
18. Raina A, Krasinskas AM, Greer JB, Lamb J, Fink E, Moser AJ, et al. Serum immunoglobulin G fraction 4 levels in pancreatic cancer: elevations not associated with autoimmune pancreatitis. Arch Pathol Lab Med 2008;132:48-53.
19. Ghazale A, Chari ST, Smyrk TC, Levy MJ, Topazian MD, Takahashi N, et al. Value of serum IgG4 in the diagnosis of autoimmune pancreatitis and in distinguishing it from pancreatic cancer. Am J Gastroenterol 2007;102:1646-1653.
20. Kamisawa T, Chen PY, Tu Y, Nakajima H, Egawa N, Tsuruta K, et al. Pancreatic cancer with a high serum IgG4 concentration. World J Gastroenterol 2006;12:6225-6228.
21. Motosugi U, Ichikawa T, Yamaguchi H, Nakazawa T, Katoh R, Itakura J, et al. Small invasive ductal adenocarcinoma of the pancreas associated with lymphoplasmacytic sclerosing pancreatitis. Pathol Int 2009;59:744-747.
22. Oh HC, Kim JG, Kim JW, Lee KS, Kim MK, Chi KC, et al. Early bile duct cancer in a background of sclerosing cholangitis and autoimmune pancreatitis. Intern Med 2008;47:2025-2028.
23. Koyabu M, Uchida K, Fukata N, Kusuda T, Ikeura T, Sakaguchi Y, et al. Primary sclerosing cholangitis with elevated serum IgG4 levels and/or infiltration of abundant IgG4-positive plasma cells. J Gastroenterol 2010;45:122-129.
24. Zen Y, Quaglia A, Portmann B. Immunoglobulin G4-positive plasma cell infiltration in explanted livers for primary sclerosing cholangitis. Histopathology 2011;58:414-422.
25. Bottazzo GF, Pujol-Borrell R, Hanafusa T, Feldmann M. Role of aberrant HLA-DR expression and antigen presentation in induction of endocrine autoimmunity. Lancet 1983;2:1115-1119.
26. Londei M, Lamb JR, Bottazzo GF, Feldmann M. Epithelial cells expressing aberrant MHC-II determinants can present antigen to cloned human T cells. Nature 1984;312:639-641.
27. Zen Y, Fujii T, Harada K, Kawano M, Yamada K, Takahira M, et al. Th2 and regulatory immune reactions are increased in immunoglobin G4-related sclerosing pancreatitis and cholangitis. HEPATOLOGY 2007; 45:1538-1546.

日消誌　2012；109：1865—1871

総　説

肝内胆管癌の腫瘍分類
—最近の展開，新たな提案を踏まえて—

中　沼　安　二[1)]

要旨：肝内胆管癌（ICC）は，肉眼的に腫瘤形成型，胆管浸潤型，胆管内発育型に分類され，発生部位から末梢型と肝門型に分けられる．末梢型 ICC の発生に，肝内小型胆管，特に細胆管～ヘリング管が関与し，肝門型 ICC は，肝門部胆管癌との鑑別が問題となる．ICC のほとんどは腺癌で，末梢型 ICC は，肝前駆細胞の形質発現がみられ，肝門型 ICC は，膵管癌に類似した形質を示す．肝門型の前癌・早期癌病変として，平坦型の胆管上皮内腫瘍（BilIN）と乳頭型の胆管内乳頭状腫瘍（IPNB）が提案された．肝の嚢胞性腫瘍は，肝粘液性嚢胞性腫瘍（MCN）と嚢胞拡張型 IPNB に分類される．

索引用語：肝内胆管癌，前癌病変，胆管上皮内腫瘍性病変

はじめに

肝内胆管癌 intrahepatic cholangiocarcinoma（ICC）は肝内胆管上皮より発生する癌腫，あるいは肝内に発生し胆管上皮に似る癌腫で，肝内胆管周囲付属腺に由来する癌腫も含める．非硬変肝に発生する例が多いが，近年，慢性ウイルス性肝炎，肝硬変に発生する例が注目され，また肝内結石症などの慢性の胆管炎や胆管傷害を背景に発生する例も知られている[1)2)]．肝細胞癌 hepatocellular carcinoma（HCC）に次いで多い肝原発の悪性腫瘍である．2010 年発刊の WHO 消化器腫瘍分類改訂版では，ICC の腫瘍分類と前癌，早期癌病変，嚢胞形成性腫瘍に関して新しい提案があり，またわが国を中心に ICC の発生機序に関する新しい病理学的見解も提案されている[3)4)]．本稿では，これらの新しい考え方を紹介し，ICC とその分類に関して述べる．

I　胆管系の解剖と ICC の定義

1．胆管系の解剖

胆管系は肝外胆管および肝内胆管に分類される．肝内胆管は，左右胆管の肝側第一次分枝に始まり，肝内大型胆管（左右胆管の第一～第三分枝程度）および肝内小型胆管に分類される[1)5)]．肝門部胆管とは一般的に，左右胆管，その合流部を指す．肝内大型胆管は肉眼的に同定が可能であり，肝内小型胆管は顕微鏡下で同定される．肝内大型胆管周囲には胆管周囲付属腺が分布する．肝内小型胆管は隔壁胆管，小葉間胆管に分類され，小葉間胆管は細胆管，ヘリング管を介して肝細胞の毛細胆管ネットワークに連続する．ヘリング管は，肝細胞と胆管上皮のハイブリッド成分である．最近の研究で，肝幹細胞/肝前駆細胞が，細胆管～ヘリング管および胆管周囲付属腺に分布することが報告され，腫瘍形成に関連するとされてい

1）金沢大学大学院医学系研究科形態機能病理学
Classification of intrahepatic cholangiocarcinoma based on recent progress and new proposal
Yasuni NAKANUMA[1)]
1）Department of Human Pathology, Kanazawa University Graduate School of Medicine
Corresponding author：中沼　安二（nakanuma@staff.kanazawa-u.ac.jp）

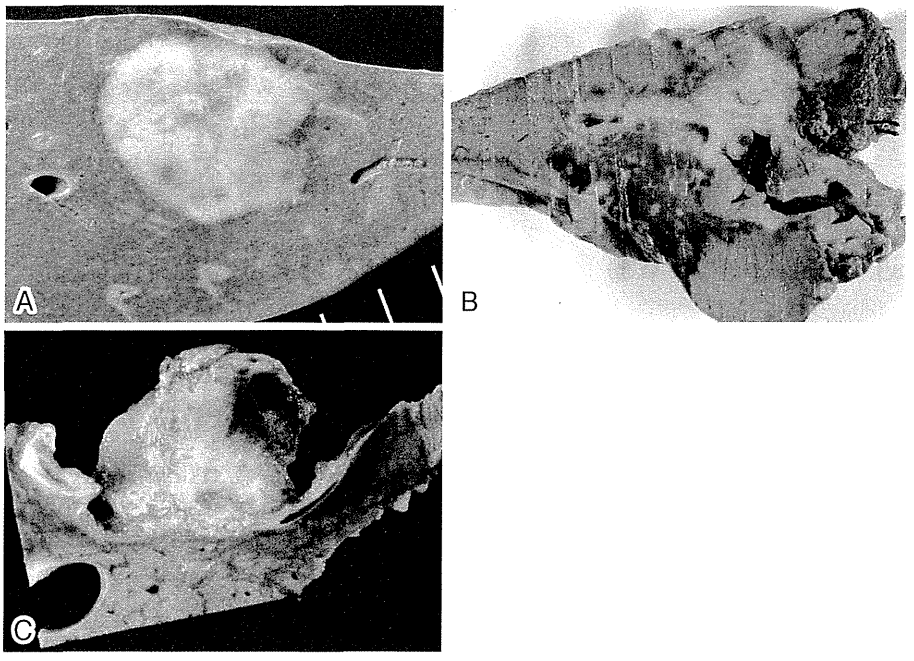

Figure 1. ICCの肉眼分類 **A**：腫瘤形成型．**B**：胆管浸潤型（肝内結石症に合併）．**C**：胆管内発育型．

る[6)~8)]．

2. ICCの定義

ICCは，左右肝管の肝側の分枝および肝実質内に発生する癌腫であり，大きく，肝末梢部に発生する末梢型peripheral ICCと，肝門部近傍の肝内胆管（胆管周囲付属腺を含む）に発生する肝門型hilar ICCがある．末梢型ICCは，肝実質内，多くは肝内小型胆管あるいは細胆管～ヘリング管から発生するICCであり，肝門型ICCは左右胆管の肝側主要分枝あるいは胆管周囲付属腺に発生し，肝門部胆管に由来する肝門部癌（分類上は肝外胆管癌あるいは胆道癌に含められる）との鑑別は，事実上困難なことが多い．そのため肝門型ICCは，肝門部癌，総肝管上部から発生する癌腫を含め，広くperihilar CC（肝門領域胆管癌，傍肝門胆管癌）として扱う試みがなされつつある[9)]．

II ICCの病理学的分類

ICCは，進行例では肝内で多発性，癒合性の腫瘍結節を形成する．現在，比較的早期で切除可能な段階で発見される症例が多くなっており，これらを対象とした肉眼分類を中心に述べる．

1. 肉眼分類

ICCは，原発性肝癌取扱い規約では，肉眼的に腫瘤形成型mass forming（MF）type，胆管浸潤型periductal infiltrating（PI）type，胆管内発育型intraductal growth（IG）typeの3型に大きく分類される（Figure 1）[1)]．この分類は現在，WHOのICCの分類にも用いられ，世界的に広く用いられつつある[2)]．末梢型ICCは腫瘤形成型の形態を示し，肝門型ICCは胆管浸潤型，胆管内発育型を呈する例が多い．

1）腫瘤形成型

肝実質に明瞭な灰白色，充実性の限局性腫瘤を形成する．腫瘍の境界は明瞭であるが，線維性の被膜形成はみられない．小数例では，周囲ににじむように浸潤し，境界がやや不明瞭となる．腫瘤形成を示すが，腫瘍部を含め，肝全体としては大きくならない．癌が周囲肝実質を取り込むように発育するためと思われる．肝臓の被膜直下に存在する腫瘤は，癌臍を形成する．末梢型ICC，細胆

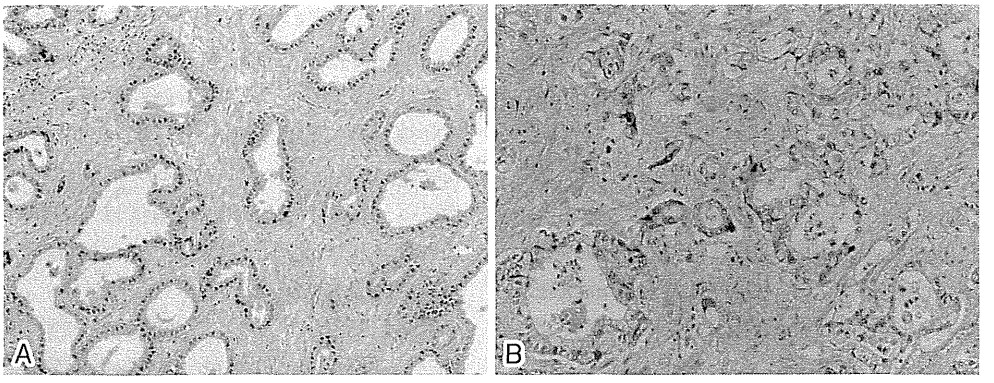

Figure 2. ICCの組織像　**A**：高分化型管状腺癌．**B**：中分化型管状腺癌．HE染色．

管あるいは肝幹細胞に由来する癌腫は，腫瘤形成型を呈する．

2）胆管浸潤型

浸潤性の胆管癌が，肝内大型胆管あるいは肝門部の胆管周囲の血管・結合組織を巻き込みつつ，胆管の長軸方向へ樹枝状進展を示し，腫瘍部胆管腔は圧排され，狭小化し，しばしば末梢胆管の拡張がみられる．しばしば周囲肝実質に向かって増殖し，結節型の形態を示し，胆管浸潤型＋腫瘤形成型に分類され，胆道癌あるいは肝門部胆管癌の平坦浸潤型，結節浸潤型[10]，あるいは欧米で用いられている nodular sclerosing type に相当する．

3）胆管内発育型

胆管内腔へ乳頭状の形態を示す癌腫であり，粘液の過剰産生を示す例が少なくなく，病変部胆管は嚢状あるいは紡錘状に拡張を示す．また，病変部胆管の拡張にともない，屈曲・蛇行し多嚢胞性の病変としてみられる例もある．多くは高分化で乳頭状発育を示し，胆管内乳頭状腫瘍 intraductal papillary neoplasm of bile duct（IPNB）の癌化に由来する例が多い．鑑別診断として，肝粘液性嚢胞性腫瘍 hepatic mucinous cystic neoplasm（肝MCN）がある．嚢胞形成性あるいは粘液産生性の胆管内発育型ICCは，胆管と交通し，また嚢胞壁に卵巣様間質はみられない．なお，二次的に拡張したICCの嚢胞性病変はMCNとしない．

2．組織像

ICCのほとんどは腺癌であり，立方上皮，低～高円柱上皮からなる管腔構造を取ることが多いが，微小乳頭状，腺房状，コード状，索状の増殖もみられ，乳頭状の増殖を示す例もある（Figure 2）．多くの例では，癌細胞は胆管上皮に似ており，サイトケラチンCK7，CK19などが陽性であり，いわゆる膵胆管上皮の表現型を示す．しばしば粘液産生を認めるが，末梢型ICCでは，粘液産生が軽度か，あるいは陰性例が多い．線維性間質がよく発達している例が多く，HCCに比べて多いが，症例により少ない例もある．高分化型，中分化型，低分化型に分けられるが，高分化型が多い[1)2)]．同一の腫瘤中で2種類以上のパターンを示す場合，量的に優勢な組織像をもって分類する．さらに特殊型（亜型）として，腺扁平上皮癌，扁平上皮癌，肉腫様癌，粘液癌，明細胞癌，印鑑細胞癌，小細胞癌，神経内分泌癌などが知られているが，いずれもまれである．

III　ICCの腫瘍分類に関する問題点

ICCは現在，その腫瘍分類，あるいは周辺の原発性肝腫瘍との鑑別や関連性においていくつかの問題点を抱えている．さらに最近，ICCの腫瘍分類に関連する，いくつかの新しい報告もなされている．これらICCの腫瘍分類での問題点を中心に解説する．

1．末梢型ICCと細胆管癌：最近の展開と混乱

1）細胆管癌とは

従来，細胆管細胞癌 cholangiolocellular carcinoma（CoCCあるいはCLC）はICCの一亜型と